ACS OMEGA

Open Access

http://pubs.acs.org/journal/acsodf

Article

One-Dimensional Defect Layer Photonic Crystal Sensor for Purity Assessment of Organic Solvents

Divya Sampath* and Venkateswaran Narasimhan

Cite This: *ACS Omega* 2024, 9, 9625−9632

Read Online

ACCESS | Metrics & More | Article Recommendations

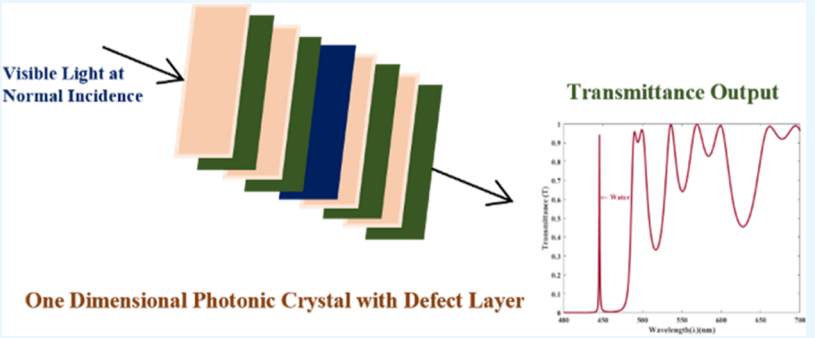

ABSTRACT: This paper presents the design and analysis of a one-dimensional defect layer photonic crystal (1D-DLPC) sensor for the assessment of the purity of chemical solvents with enhanced accuracy. Chemical solvents are frequently used in chemical processes as reaction mediums. It is essential to ascertain its purity since impurities can significantly affect the outcome of the reaction. The structure of the proposed one-dimensional defect layer photonic crystal sensor consists of a defect layer sandwiched between alternate layers of ZnO and SiO_2 organized with a certain periodicity. It has been shown that the localized defect modes inside the structure can detect minute refractive index changes based on the degree of impurity of chemical solvents. Simulation studies have been performed through the transfer matrix method (TMM) and the performance of the design is evaluated using several metrics such as sensitivity, full width at half-maximum, figure of merit, quality factor, and dynamic range. Results indicate that the designed one-dimensional defect layer photonic crystal sensor has a significantly high efficiency and is suitable for detecting impure solvents.

1. INTRODUCTION

Since the emergence of photonic crystals in the early 1990s, various exciting applications have been researched across different fields. These crystals manipulate light flow like semiconductors controlling electron flow engineered at light wavelength scales. Photonic crystals consist of a periodic structure of materials, creating a band gap that prevents certain frequencies of light from propagating through the material. It finds numerous applications in both science and technology, such as optics, photonic integrated devices, light-emitting diodes (LEDs), lasers, biosensors, and chemical sensors, etc. In Photonic crystals, reflectance, transmittance, band structure, group velocity, and the rate of spontaneous emission are a few features that are considerably altered by the periodic modification of the refractive index.[1]

This paper presents a one-dimensional defect layer photonic crystal crafted specifically to track the displacement of the defect mode within the photonic band gap. The primary objective is to assess the purity of chemical solvents through this innovative design. We investigated a one-dimensional defect layer photonic crystal (1D-DLPC) with a defect layer positioned between alternating ZnO and SiO_2 layers.[2,3] Using physical vapor deposition (PVD) or chemical vapor deposition (CVD) techniques, the layers of the photonic crystal can be fabricated. During the fabrication process, the defect layer can be introduced as a cavity, where the solvent can be used. This cavity can be created by omitting the deposition of material in that specific region or etching away material. This photonic crystal structure can further be optimized to identify minute variations in the refractive index brought about by introducing contaminants in the acetone−water mixture through the localized fault modes.[4]

Traditional methods for assessing the purity of organic substances, such as solvate chromic fluorescence probes,

Received: December 1, 2023
Revised: January 18, 2024
Accepted: January 25, 2024
Published: February 12, 2024

https://doi.org/10.1021/acsomega.3c09589
ACS Omega 2024, 9, 9625−9632

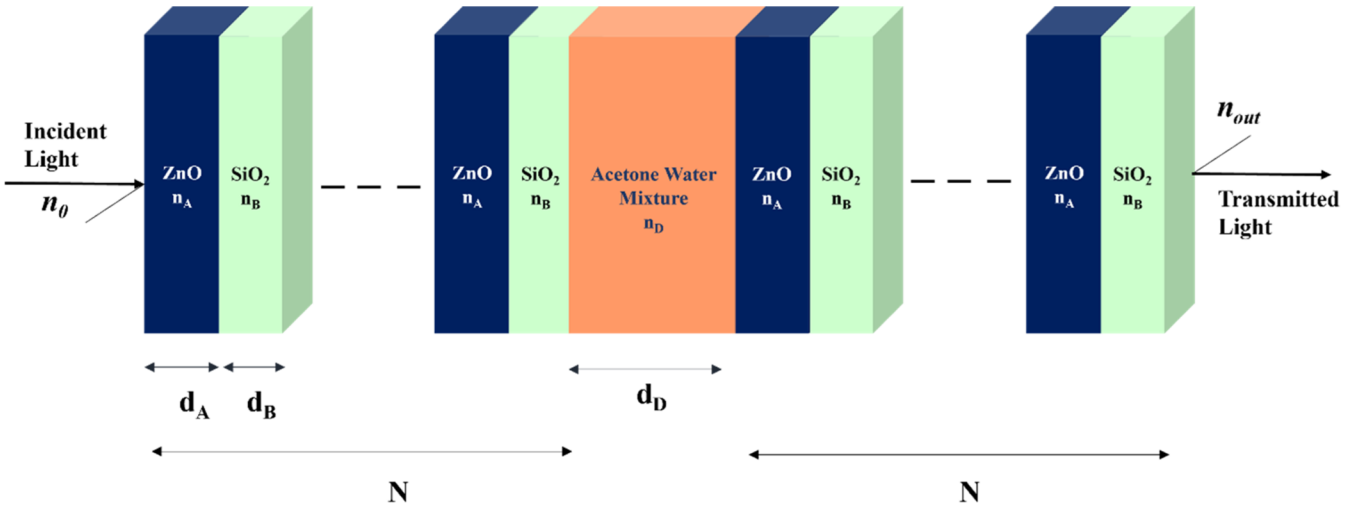

Figure 1. Design of the chemical sensor based on the one-dimensional defect layer photonic crystal structure.

electronic noses, quartz crystal microbalances, solvent-response materials, and chromatography−mass spectrometry, often involve complex setups, are challenging to use, expensive, and time-consuming.[5,6] In response to these challenges, there is growing interest in alternative detection technologies. One promising approach is photonic crystal (PC) based detection, leveraging the powerful sensing and detection capabilities of photonic crystals. These periodic optical nanostructures possess an exceptional capability of sensing organic compounds by selectively capturing alterations in the refractive index. One-dimensional defective photonic crystals, among other photonic crystal structures, present a standout advantage due to their simpler, cost-effective fabrication compared to higher-dimensional models. This characteristic renders them highly compelling for pioneering efficient detection technologies.[7] The inclusion of a defect layer within the one-dimensional photonic crystal structure leverages the distinct optical characteristics of acetone and water to discern the purity of a mixture. The Transfer Matrix Method (TMM) is a widely used technique for the investigation of complicated multilayer structures, including photonic crystals.[8] The method is well suited to layered structures with varying properties. Compared to the Finite Difference Time Domain (FDTD) and Finite Element Method, TMM is simple when the entire structure interacts only with adjacent layers with a repeating pattern.

The structure of the proposed work is as follows: The design and optimization of the 1D defect layer photonic crystal (1D-DLPC) structure are presented in Section 2. The measurement of the refractive index of the acetone−water mixture is covered in Section 4. The many performance measures used to assess the organic sensor are covered in Section 5. The simulation results are shown in Section 6, and the conclusions are shown in Section 7.

2. DESIGN AND OPTIMIZATION OF THE ONE-DIMENSIONAL DEFECT LAYER PHOTONIC CRYSTAL (1D-DLPC)

To assess solvent purity, we explored the application of a conventional one-dimensional defect layer photonic crystal structure. This structure comprises alternating layers of two dielectric types, each with distinct thickness and dielectric constant values while maintaining a constant spatial period. We assume uniformity and an infinite extension of each layer along the length and width dimensions. The term "one-dimensional" describes the variation of the dielectric function solely along a single dimension. Photonic crystals, periodic or quasiperiodic, possess lattice dimensions comparable to light wavelengths. Interaction with these structures leads to the formation of bandgaps for distinct light wavelengths.[9] Fabricating cavity-based photonic chemical sensors of this nature is achievable using commonly available thin-film methods such as spin-coating and dip-coating.[10]

The design parameter of the defect layer between two symmetric one-dimensional sub-PCs has alternating layers of ZnO and SiO_2 with refractive indices of $n_A = 2.003$ and $n_B = 1.45$, respectively. For, small values of $\frac{\Delta n}{n_A}$, $\Delta n = n_A - n_B$, many works of literature present more general design equations that maximize the band gap.[11] From Figure 1, it was shown that for the two materials with refractive indices (n_A and n_B) and thicknesses d_A and d_B respectively, for the normal incidence, the band gap is maximized when $d_A n_A = d_B n_B$ or, equivalently, $d_A = a n_C \frac{n_A}{n_B}$, where $a = d_A + d_B$ and n_c = effective refractive index. In this case, it can be shown that the midband frequency ω_m is $\omega_m = \left(\frac{n_A + n_B}{(4n_A n_B)}\right)\left(\frac{2\pi c}{a}\right)$ where c = velocity of light in free space. Thus, the ZnO and SiO_2 layers have thicknesses of $d_A = 52$ nm and $d_B = 72$ nm, respectively. The choice of periodicity is optimized to obtain deep transmission minima.

Localized states emerge within the band gap of a photonic crystal upon introduction of a discontinuity in its periodic arrangement, akin to electronic bandgaps in semiconductors. The thickness of the defect layer governs the resonance wavelength, confining light within the flaw. Altering this thickness impacts the initial band gap and, consequently, the range of wavelengths the crystal can transmit or reflect.[12,13] It may also influence guided light's group velocity and dispersion. Simulation helps identify the optimal defect layer thickness to achieve the desired performance.

3. THEORETICAL FORMULATION OF THE TRANSFER MATRIX METHOD (TMM)

The transfer matrix method is a robust mathematical technique employed to analyze the transmission of light through a photonic crystal containing multiple layers with distinct optical

https://doi.org/10.1021/acsomega.3c09589
ACS Omega 2024, 9, 9625−9632

properties.[14,15] This method operates under the assumption that the optical properties remain constant and are known within each layer. Additionally, it presupposes that the light wave can be expressed as a combination of plane waves propagating within the material. For every layer, a 2 × 2 transfer matrix, also termed the propagation matrix, is constructed to characterize the optical properties specific to that layer. This transfer matrix establishes a connection between the incoming wave amplitudes and the outgoing wave amplitudes at each interface and can be expressed as follows

$$M_k = \begin{bmatrix} \cos \rho_k & \left(-\frac{i}{\varphi_k}\right)\sin \rho_k \\ -i\varphi_k \sin \rho_k & \cos \rho_k \end{bmatrix} \quad (1)$$

where, k denotes various layers A, B, and C.

ρ_k is defined as

$$\rho_k = \frac{2\pi}{\lambda} d_k n_k \cos \theta_k$$

where, d_k, n_k, and θ_k signify the thickness, refractive index, and angle of incidence of the kth layer, respectively. Free space wavelength is denoted as λ. ϕ_k is defined as $\phi_k = Z_0 n_k \cos \theta_k$ for TE mode and $\phi_k = \frac{\cos \theta_k}{Z_0 n_k}$ for TM mode, where z_0 is the free space impedance.

To find the overall transfer matrix for the entire structure, the transfer matrices of all the individual layers are simply multiplied together. The transfer matrix of the complete structure is

$$M = \begin{bmatrix} M_{11} & M_{12} \\ M_{21} & M_{22} \end{bmatrix} = (M_A M_B)^N M_D (M_A M_B)^N \quad (2)$$

Here, M_A, M_B, and M_D represent the transfer matrix ZnO, SiO_2, and defect layer.

The transmittance coefficient and reflectance coefficient are given by

$$t = \frac{2\gamma_0}{(M_{11} + \gamma_y M_{12})\gamma_0 + (M_{21} + \gamma_y M_{22})} \quad (3)$$

$$r = \frac{(M_{11} + \gamma_y M_{12})\gamma_0 - (M_{21} + \gamma_y M_{22})}{(M_{11} + \gamma_y M_{12})\gamma_0 + (M_{21} + \gamma_y M_{22})} \quad (4)$$

where γ_0 and γ_y signify the impedance of the incident and output medium of the proposed structure. In the case of TE polarized light, γ_0 and γ_y is given by $\gamma_0 = Z_0 n_0 \cos \theta_{in}$ and $\gamma_y = Z_0 n_y \cos \theta_y$. Here Z_0 represents the free space impedance. Once the overall transfer matrix is obtained, the reflectance (R) and transmittance (T) of the proposed one-dimensional photonic crystal can be calculated from

$$T = \frac{n_0}{n_{out}} |t^2| \quad (5)$$

$$R = |r|^2 \quad (6)$$

Absorption (A) of the multilayer structure can be given as

$$A = 1 - T - R$$

where n_0 is the refractive index of the input medium.

n_{out} is the refractive index of the output medium, either air or any other substrate.

Transfer matrix method (TMM) was simulated in MATLAB R2023, to evaluate the performance. The advantage of 1D-DLPC simulations in MATLAB is that they can shorten and lower the experimental testing time.

4. ESTIMATION OF THE REFRACTIVE INDEX OF THE ACETONE−WATER MIXTURE

Estimating the refractive index of acetone/water mixtures holds significance across various scientific disciplines due to the indispensability of organic solvents. These solvents play vital roles in chemistry, biology, pharmacology, and materials science, facilitating material extraction, suspension, and dissolution.[16,17] They serve as crucial reaction media in chemical operations, ensuring reactant dissolution, homogeneous reactions, and controlled reaction rates. Laboratories rely on solvents for tasks like dilution, chromatography, and sample preparation, while industrial settings utilize various organic solvents like isopropyl alcohol, trichloroethylene, and perchloroethylene for effective degreasing and cleaning processes.[18]

In liquid−liquid mixtures, which are used in many industrial applications, the refractive index is an important tool for indirectly determining their purity. The degree of reflection and light transmission through a material are both strongly impacted by the purity of the substance.[19,20] Reduced transmittance can occur from light absorption and scattering caused by contaminants. This study explores the correlation between a material's transmittance and its refractive index, specifically examining the effects of varying acetone concentrations on these properties. Distilled water and pure acetone exhibit refractive indices of 1.333 and 1.3586, respectively. The investigation centers on acetone−water mixtures, encompassing concentrations from 20 to 80%. The mixing process induces structural reorientation attributed to differences in component shape, size, and intermolecular interactions. The purity of acetone substantially impacts its optical traits and usability.[21]

Many pure liquids have refractive index values that are either well-known or easily accessible in the literature. Nevertheless, interferometric or deflection methods are usually employed to ascertain the refractive indices of a binary liquid combination.[20] Refractometers are used in deflection procedures to determine the refractive index using the critical angle effect. Abbe refractometers, inline process refractometers, conventional hand-held refractometers, and digital hand-held refractometers are the four basic types of refractometers.[22,23] In general, an Abbe refractometer can be used to evaluate the refractive indices of water and acetone mixtures, providing an accurate measurement. As an alternative, an exact mixing rule can be used to estimate the refractive index from pure components.

The refractive indices of pure components and their mixes were determined across various temperatures and volume fractions, validating established mixing laws as outlined by Nowakowska J. et al.[24] The Arago-Biot relation, based on volume additivity during mixing, stands as the simplest approximation to the true values for binary mixtures, offering a foundational perspective in this regard. It is stated as

$$n_m = n_1 y_1 + n_2 y_2 \quad (7)$$

where, n_m = refractive index of the mixture

n_1, n_2 = refractive index of pure components

y_1, and y_2 = volume fractions

https://doi.org/10.1021/acsomega.3c09589
ACS Omega 2024, 9, 9625−9632

The calculated estimated refractive indices using the straightforward Arago-Biot relation exhibit significant variations across different volume fractions in Table 1. This variation highlights the substantial change in refractive indices within the mixtures, as derived from eq 7. The Arago-Biot mixing rule's advantage lies in its simplicity and extensive applicability across various scenarios, distinguishing it from other relations discussed in the literature.

Table 1. Refractive Index of Water and Acetone Mixture Concentration

s. no	concentration of impurity of acetone (%)	refractive index (n)
1	0% (pure acetone)	1.3586
2	20%	1.3548
3	40%	1.3484
4	60%	1.3432
5	80%	1.3381
6	100%	1.3330

5. PERFORMANCE METRICS FOR THE EVALUATION OF THE CHEMICAL SENSOR

This section delves into a few crucial parameters that are necessary to assess the suggested sensor's performance. Quantitatively assessing performance involves examining various metrics like sensitivity (S), figure of merit (FoM), quality factor (QF), and dynamic range (DR).[25,26] Sensitivity (S) is determined by observing the shift in the peak position of the defect mode caused by the influence of impure acetone/water mixtures on the refractive index. The following is a way to express this sensitivity

$$S = \frac{\lambda_D}{n_D} \tag{8}$$

An additional quantitative indicator used to evaluate the performance of the suggested sensor is called the "Figure of Merit" (FoM). The ratio of the spectral width at half-maximum to the value of the peak resonant wavelength is used to calculate this statistic. The FoM is defined as

$$\text{FoM} = \frac{S}{\text{FWHM}} \tag{9}$$

fwhm, which stands for "Full Width at Half Maximum", is commonly utilized to characterize the spectral resolution of a sensor. It represents the bandwidth of the sensor's response, indicating the range over which the sensor can effectively detect signals. A narrower fwhm generally signifies a higher sensitivity and a higher Figure of Merit (FoM), enabling the sensor to detect smaller changes in the input signal.

The Quality Factor (Q_f) serves as a metric for the energy stored in the photonic crystal cavity relative to the energy lost through dissipative mechanisms such as absorption and scattering. It quantifies the effectiveness of the photonic crystal in trapping and storing light within the resonator. Minimizing losses attributed to scattering, absorption, and fabrication imperfections contribute to an increased Quality factor.

A higher Quality Factor suggests that the photonic crystal cavity excels in efficiently detecting changes in the refractive index of the surrounding environment. Mathematically, the Quality Factor (Q_f) can be defined as

$$Q_f = \frac{\lambda_D}{\text{FWHM}} \tag{10}$$

Where λ_D is the resonant frequency of the cavity mode (the frequency at which the cavity strongly interacts with light). $\Delta\omega$ is the full width at half-maximum (fwhm) of the resonant peak in the photonic crystal's transmission or reflection spectrum.

The dynamic range (DR) of a 1D photonic crystal refers to the difference between maximum and minimum input power levels that a photonic crystal device can operate effectively and accurately. It is calculated using the relation,

$$\text{DR} = \frac{\lambda_D}{\sqrt{\text{FWHM}}} \tag{11}$$

The design is aimed at a broader dynamic range performance by optimizing the device's structure.

6. SIMULATION RESULTS AND DISCUSSION

6.1. Evaluation of the Refractive Index and Transmittance of the Acetone−Water Mixture Samples. In this section, the performance of the proposed design was evaluated concerning variations in the refractive indices of the acetone−water mixture, periodicity, and thickness of the defect layer. This evaluation was conducted by analyzing the transmittance spectra at normal incidence. A crucial physical parameter for assessing the purity of any solvent is its refractive index.[27,28] The refractive indices of pure acetone and water, along with their respective proportions, determine the refractive index of the mixture. At a specific temperature of 30 °C, the refractive indices of the acetone and water mixtures were determined using the Arago-Biot relation and are presented in Table 1.

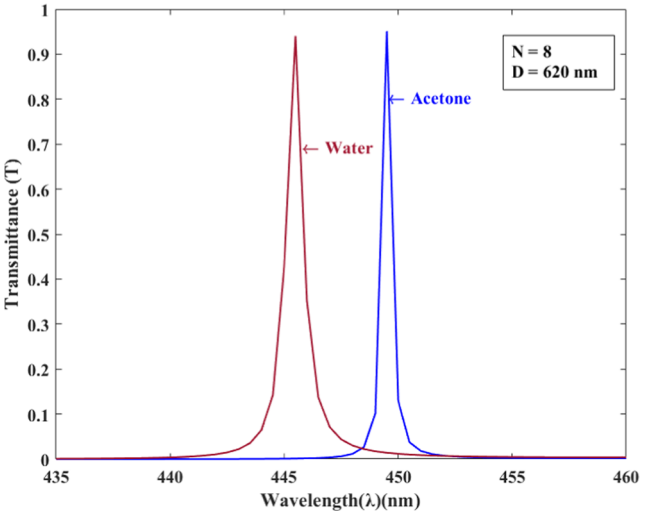

Figure 2. Transmittance spectra of water and acetone with refractive index at normal incidence in a $(\text{ZnO SiO}_2)^N$ defect layer $(\text{ZnO SiO}_2)^N$ sensor with defect layer thickness d_D = 620 nm and periodicity N = 8.

Water and acetone molecules possess distinct molecular structures and polarities. When mixed, water molecules interact with acetone molecules through dipole−dipole interactions and hydrogen bonding. These interactions cause the local electric fields around the molecules to align, resulting in an increase in the effective refractive index of the mixture compared to that of water alone. A higher refractive index in pure acetone indicates that light travels slower in the defect cavity.[28,29]

https://doi.org/10.1021/acsomega.3c09589
ACS Omega 2024, 9, 9625−9632

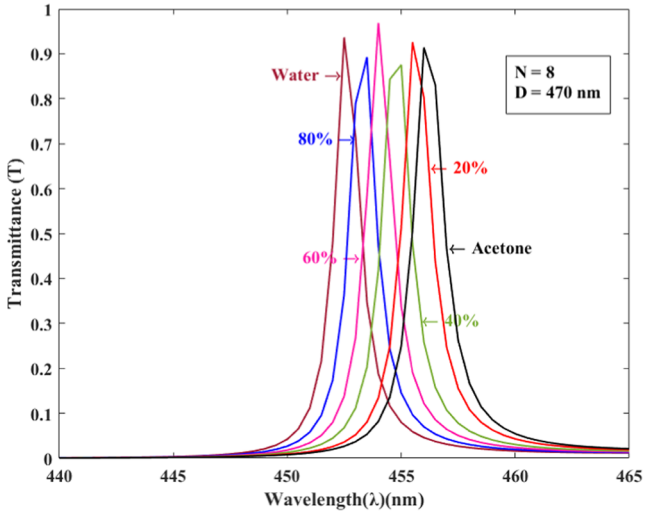

(a)

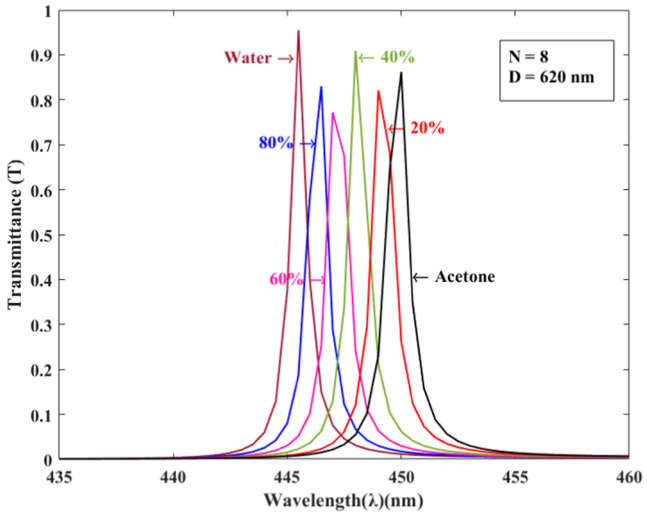

(b)

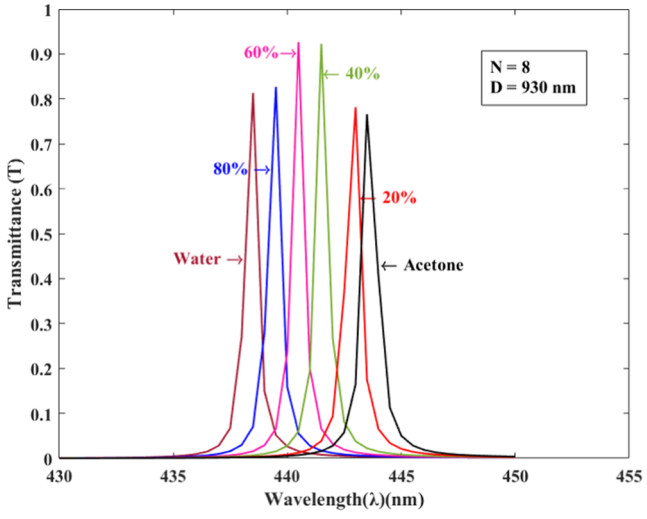

(c)

Figure 3. Transmittance spectra of the different defect layer thickness at normal incidence in a $(ZnO\ SiO_2)^N$ defect layer $(ZnO\ SiO_2)^N$ sensor with (a) d_D = 470 nm. (b) d_D = 620 nm and (c) d_D = 930 nm.

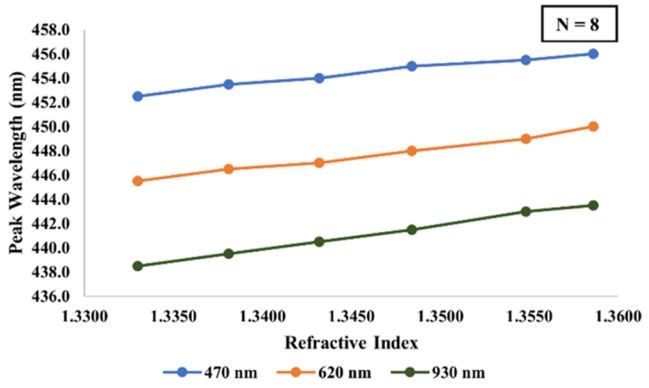

(a)

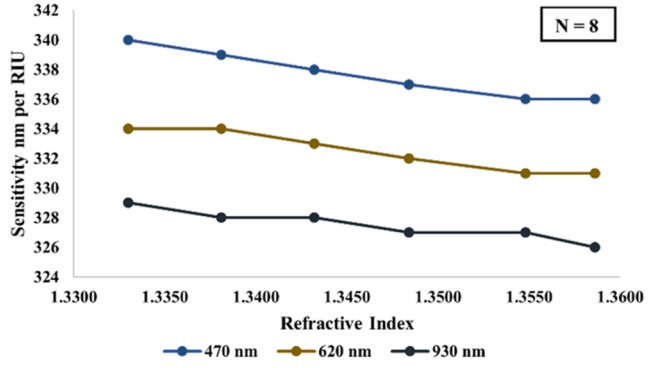

(b)

Figure 4. (a) Peak wavelength and (b) sensitivity of resonant modes associated with defect layer thickness at normal incidence in a $(ZnO\ SiO_2)^N$ defect layer $(ZnO\ SiO_2)^N$ sensor has different defect layer thickness d_D = 470 nm, d_D = 620 nm, and d_D = 930 nm for N = 8.

Further, the proposed sensor is evaluated for the transmittance spectra of the mixture of acetone−water at various compositions at normal incidence simulated using the MATLAB simulation tool. The transmittance of the $(ZnO\ SiO_2)^N$ defect layer $(ZnO\ SiO_2)^N$ photonic crystal sensor has been evaluated using the TMM. Initially, the thickness of d_1 and d_2 was arrived using the design formulas presented in Section 4, as 52 and 72 nm, respectively. The periodicity of the layers considered is N = 8. Using a water sample in the defect layer, the transmittance is depicted in Figure 2. The observed resonance within the photonic band gap reveals a distinctive feature known as the defect resonant mode, stemming from the perturbation within the structure's periodicity. Figure 3 demonstrates a defect mode with 94% transmittance, notably centered at a wavelength of 445.5 nm. Additionally, the transmittance spectra within the photonic band gap exhibit some high-transmittance ripples, notably on the higher wavelength side. Since the cavity region is in the middle of the design, the two identical $(ZnO\ SiO_2)^N$ sub-PCs on either side of it serve as identical Bragg mirrors. Localized defect modes are a result of light being able to bounce back and forth in the area between the two Bragg mirrors.

6.2. Evaluation of the Performance of the $(ZnO\ SiO_2)^N$ Defect Layer $(ZnO\ SiO_2)^N$ Sensor for different Thicknesses of the Defect Layer. The effect of change in defect layer thickness with d_D = 620 nm, d_D = 470 nm, and d_D = 930 nm was studied on the transmission properties. Figure 3 shows the

https://doi.org/10.1021/acsomega.3c09589
ACS Omega 2024, 9, 9625−9632

Table 2. Peak Wavelength, Transmittance, and Sensitivity of Resonant Modes for different Defect Layer Thickness at Normal Incidence in a $(ZnO\ SiO_2)^N$ Defect Layer $(ZnO\ SiO_2)^N$ Sensor

	d_D = 470 nm			d_D = 620 nm			d_D = 930 nm		
refractive index of the mixture	wavelength (nm)	transmittance (T)	sensitivity nm per RIU	wavelength (nm)	transmittance (T)	sensitivity nm per RIU	wavelength (nm)	transmittance (T)	sensitivity nm per RIU
1.3586	456.0	0.9317	336	450.0	0.8621	331	443.5	0.6665	326
1.3548	455.5	0.9257	336	449.0	0.8208	331	443.0	0.8269	327
1.3484	455.0	0.8752	337	448.0	0.8754	332	441.5	0.9262	327
1.3432	454.0	0.9682	338	447.0	0.7720	333	440.5	0.8660	328
1.3381	453.5	0.8924	339	446.5	0.8300	334	439.5	0.7814	328
1.3330	452.5	0.9364	340	445.5	0.9403	334	438.5	0.7659	329

Table 3. Wavelength and Sensitivity of Resonant Modes at Normal Incidence in a $(ZnO\ SiO_2)^N$ Defect Layer $(ZnO\ SiO_2)^N$ Sensor for Various Periodicity N = 4, N = 6, and N = 8

	N = 4			N = 6			N = 8		
refractive index of the mixture	wavelength (nm)	transmittance (T)	sensitivity nm per RIU	wavelength (nm)	transmittance (T)	sensitivity nm per RIU	wavelength (nm)	transmittance (T)	sensitivity nm per RIU
1.3586	453.0	0.9517	333	450.5	0.9378	332	450.0	0.8621	331
1.3548	452.5	0.9524	334	450.0	0.9563	332	449.0	0.8208	331
1.3484	451.0	0.9506	334	449.0	0.9516	333	448.0	0.8754	332
1.3432	450.0	0.9507	335	448.0	0.9533	334	447.0	0.7720	333
1.3381	449.0	0.9504	336	447.0	0.9538	334	446.5	0.8300	334
1.3330	448.0	0.9492	336	446.0	0.9463	335	445.5	0.9403	334

Table 4. Performance of the Proposed $(ZnO\ SiO_2)^N$ Defect Layer $(ZnO\ SiO_2)^N$ Sensor with Defect Layer Thickness 620 nm

	fwhm (nm)			FoM (nm per RIU)			quality factor (Q_f)			dynamic range (DR)		
refractive Index of the mixture	N = 4	N = 6	N = 8	N = 4	N = 6	N = 8	N = 4	N = 6	N = 8	N = 4	N = 6	N = 8
1.3586	0.0615	0.0505	0.0486	5415	6574	6815	7366	8920	9259	1827	2005	2041
1.3548	0.0645	0.0598	0.0476	5178	5552	6962	7016	7525	8804	1781	1840	1988
1.3484	0.0635	0.0615	0.0496	5259	5415	6694	7102	7300	9032	1790	1811	2012
1.3432	0.0625	0.0589	0.0485	5360	5660	6866	7200	7606	8994	1800	1846	2005
1.3381	0.0618	0.0628	0.0483	5437	5321	6907	7265	7118	8842	1806	1784	1986
1.3330	0.0632	0.0565	0.0500	5316	5929	6680	7088	7893	8910	1782	1876	1992

transmittance characteristics of the mixture of water and acetone with a range of refractive indexes of 1.3330−1.3586. As the thickness is increased from d_D = 470 nm, the sequence of discrete modes pulls down into the gap from the upper bands for different impurity values.

Table 2 illustrates the changes in the refractive index of the mixture, peak resonant position, transmittance, and sensitivity of the resonant modes associated with three distinct defect layer thicknesses. The analysis reveals that the peak wavelength consistently decreases as the concentration shifts from pure to impure for all three defect layer thicknesses. Concurrently, an increase in defect layer thickness corresponds to a decrease in transmittance. However, it can be noted from Figure 4a,b that the relationship between refractive index vs peak wavelength and refractive index vs sensitivity seems to follow certain linearity but can vary with temperature and other factors. Better Sensitivity measure is observed for resonant modes with d_D = 620 nm for N = 8.

6.3. Performance of the Proposed $(ZnO\ SiO_2)^N$ Defect Layer $(ZnO\ SiO_2)^N$ Sensor for different Period Number (N). Investigations have been performed to study the transmission characteristics of the proposed multilayer sensor. change as the number of periods changes from N = 4 to N = 10 in steps of two.

Figure 5 shows the transmittance spectra and peak wavelength of resonant modes at normal incidence in a $(ZnO\ SiO_2)^N$ Defect layer $(ZnO\ SiO_2)^N$ sensor associated with N = 4, N = 6, and N = 8 for defect layer thickness equal to 620 nm. Table 3 distinctly illustrates the resonant mode wavelength shifting toward the lower band with increased periodicity, consequently leading to reduced transmittance. Furthermore, the sensitivity measure of resonant modes indicates the sensor's capability to uniformly detect and respond to changes in the periodicity parameter N.

Figure 6a,b shows the correlation between the refractive index and peak wavelength, as well as the refractive index and sensitivity. This appears to exhibit a degree of linearity. However, it is noteworthy that this relationship may exhibit variations influenced by factors such as temperature and others. A higher sensitivity measure is observed for resonant modes with a defect layer thickness (d_D) of 620 nm when the number of layers (N) is equal to 8.

6.4. Performance Analysis of the Proposed $(ZnO\ SiO_2)^N$ Defect Layer $(ZnO\ SiO_2)^N$ Sensor. The performance of the proposed sensor has been assessed using several standard metrics, including Full Width at Half Maximum (fwhm), figure of merit (FoM), quality factor (QF), and dynamic range (DL) for two distinct values of the periodicity parameter.[29] The results are summarized in Table 4. It is evident that a narrower fwhm is achieved for N = 8. Additionally, higher FoM values for N = 8 suggest that the designed sensor exhibits increased sensitivity, enabling the detection of smaller changes in the input signal.

https://doi.org/10.1021/acsomega.3c09589
ACS Omega 2024, 9, 9625−9632

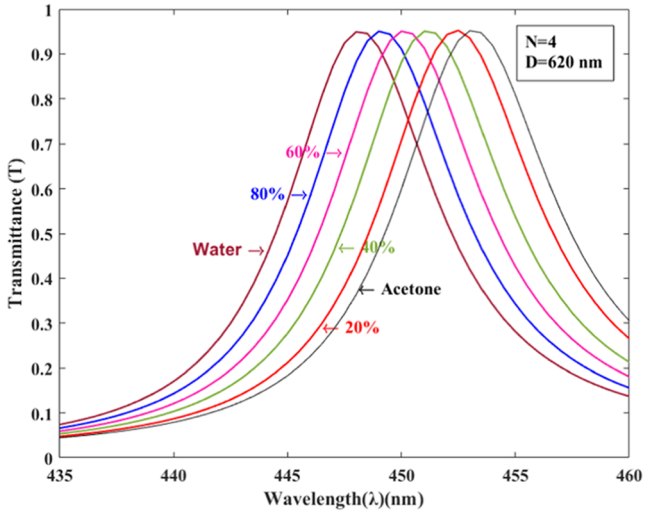

(a)

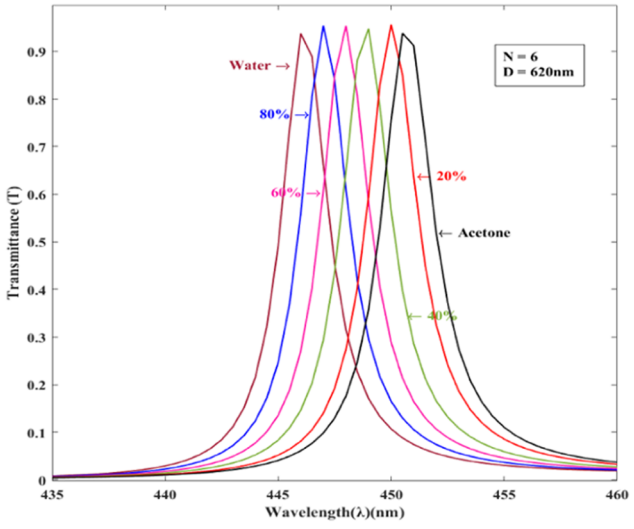

(b)

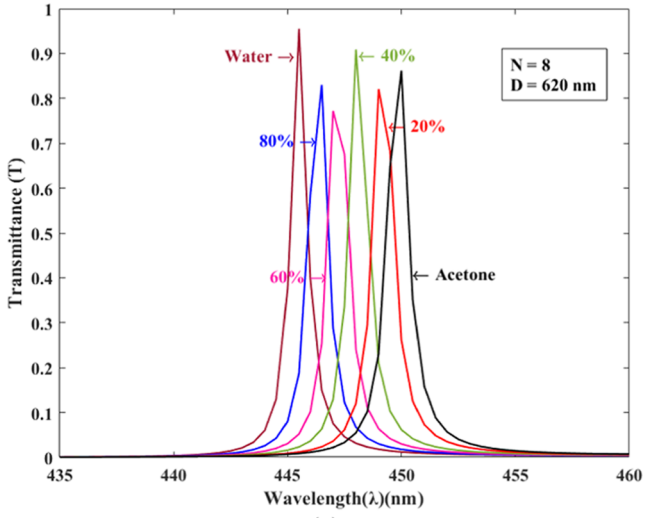

(c)

Figure 5. Transmittance spectra and resonant wavelength at normal incidence in a $(ZnO\ SiO_2)^N$ Defect layer $(ZnO\ SiO_2)^N$ sensor for various periodicities (a) $N = 4$, (b) $N = 6$ and (c) $N = 8$.

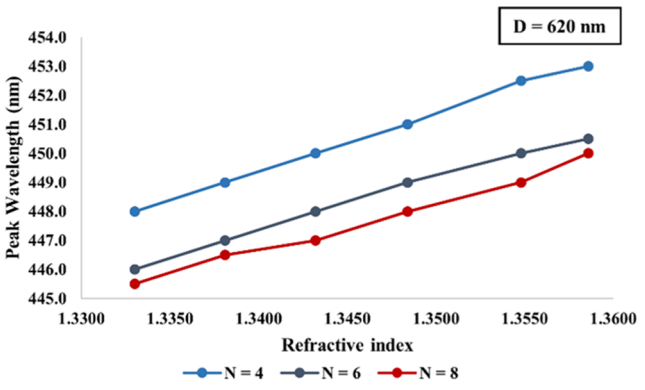

(a)

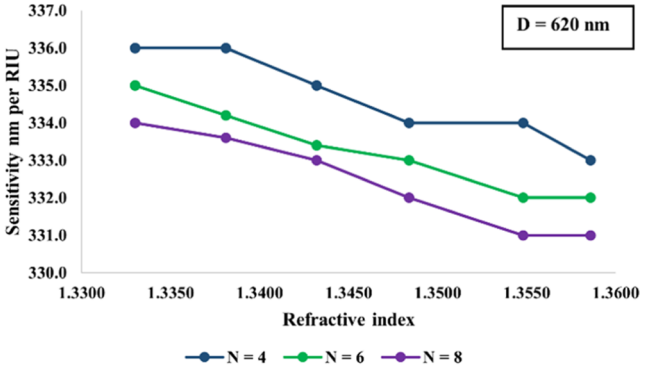

(b)

Figure 6. (a) Peak wavelength and (b) Sensitivity of resonant modes at normal incidence in a $(ZnO\ SiO_2)^N$ Defect layer $(ZnO\ SiO_2)^N$ sensor for various associated with defect layer thickness $d_D = 470$ nm, $d_D = 620$ nm, and $d_D = 930$ nm for $N = 8$.

The Quality factor quantifies the sharpness of the resonance peak. As depicted in Table 4, a higher Quality factor for $N = 8$ indicates heightened sharpness and selectivity in the sensor's response near its resonant wavelength. This denotes an increased efficacy in detecting impurity levels with minimal changes in the refractive index. Moreover, at $N = 8$, a higher dynamic range is evident, suggesting the sensor's ability to function across a wide range of signal levels and detect weak signals, even amid substantial variations in the input signal.

7. CONCLUSIONS

In this paper, the design and analysis of a one-dimensional photonic crystal sensor $(ZnO\ SiO_2)^N$ Defect layer $(ZnO\ SiO_2)^N$ are aimed to detect impurities in acetone−water mixtures by monitoring minute refractive index variations. Employing the transfer matrix method, the investigation delves into transmittance concerning impurity levels, considering fluctuations in defect layer thickness, periodicity, and impurity concentrations. Simulation outcomes validate the efficacy of the proposed sensor design, showcasing optimized parameters: ZnO and SiO_2 layer thicknesses of 52 and 72 nm, defect layer thickness of 620 nm, and $N = 8$. This configuration exhibits exceptional quality and efficacy in discerning the purity levels of acetone−water mixtures. The research findings bear substantial implications for propelling advancements in photonic sensors, particularly within the chemical industry and various related applications.

https://doi.org/10.1021/acsomega.3c09589
ACS Omega 2024, 9, 9625−9632

AUTHOR INFORMATION

Corresponding Author

Divya Sampath − *Department of Biomedical Engineering, Sri Sivasubramaniya Nadar College of Engineering (Autonomous), Chennai 603110 Tamil Nadu, India;* orcid.org/0009-0001-0528-6031; Email: sdivya@ssn.edu.in

Author

Venkateswaran Narasimhan − *Department of Biomedical Engineering, Sri Sivasubramaniya Nadar College of Engineering (Autonomous), Chennai 603110 Tamil Nadu, India*

Complete contact information is available at: https://pubs.acs.org/10.1021/acsomega.3c09589

Notes

The authors declare no competing financial interest.

ACKNOWLEDGMENTS

Authors acknowledge the management, Department of ECE, and Department BME of Sri Sivasubramaniya Nadar College of Engineering (Autonomous), OMR, Kalavakkam, Chennai 603110, Tamil Nadu, India for their support.

REFERENCES

(1) Sukhovanov, A.; Guryev, I. V. *Photonic Crystals Physics and Practical Modelling*; Springer Series in Optical Science: New York, 2009.

(2) Irimpan, L.; Krishnan, B.; Nampoori, V. P. N.; Radhakrishnan, P. Linear and nonlinear optical characteristics of ZnO−SiO_2 nanocomposites. *Appl. Opt.* **2008**, *47* (24), 4345−4351, DOI: 10.1364/ao.47.004345.

(3) Uniyal, A.; Srivastava, G.; Pal, A.; Taya, S.; Muduli, A. Recent advances in optical biosensors for sensing applications: A review. *Plasmonics* **2023**, *18*, 735−750, DOI: 10.1007/s11468-023-01803-2.

(4) Al-Dossari, M.; Awasthi, S.; Mohamed, A.; et al. Bio-alcohol sensor based on one-dimensional photonic crystals for detection of organic materials in wastewater. *Materials* **2022**, *15*, No. 4012, DOI: 10.3390/ma15114012.

(5) Bolz, C. D.; Wahl, K. L.; Wahl, J. H. Investigating Solvent Purity Using Comprehensive Gas Chromatography: A Study of Acetone. *LCGC Europe* **2010**, *23* (4), 188−199.

(6) Pauli, G. F.; Chen, S.-N.; Simmler, C.; Lankin, D. C.; Gödecke, T.; Jaki, B. U.; Friesen, J. B.; McAlpine, J. B.; Napolitano, J. G. Importance of Purity Evaluation and the Potential of Quantitative 1H NMR as a Purity Assay. *J. Med. Chem.* **2014**, *57* (22), 9220−9231, DOI: 10.1021/jm500734a.

(7) Bijalwan, A.; Singh, B. K.; Rastogi, V. Analysis of one-dimensional photonic crystal-based sensor for detection of blood plasma and cancer cells. *Optik* **2021**, *226*, No. 165994.

(8) Matar, Z. S.; Al-Dossari, M.; Awasthi, S. K.; Mohamed, D.; Abd El-Gawaad, N. S.; Aly, A. H. for Conventional Biophotonic Sensing Approach for Sensing and Detection of Normal and Infected Samples Containing Different Blood Components. *Crystals* **2022**, *12*, No. 650, DOI: 10.3390/cryst12050650.

(9) Aly, A. H.; Awasthi, S. K.; Mohamed, D.; et al. Study on a one-dimensional defective photonic crystal suitable for organic compound sensing applications. *RSC Adv.* **2021**, *11*, 32973−32980.

(10) Hlubina, P.; Gryga, M.; Ciprian, D.; Pokorny, P.; Gembalova, L.; Sobota, J. High performance liquid analyte sensing based on Bloch surface wave resonances in the spectral domain. *Opt. Laser Technol.* **2022**, *145*, No. 107492.

(11) Şimşek, S. A novel method for designing one-dimensional photonic crystal with given bandgap characteristics. *AEU Int. J. Electron. Commun.* **2013**, *67* (10), 827−832.

(12) Gryga, M.; Ciprian, D.; Gembalova, L.; Hlubina, P. One-Dimensional Photonic Crystal with a Defect Layer Utilized as an Optical Filter in Narrow Linewidth LED-Based Sources. *Crystals* **2023**, *13*, No. 93, DOI: 10.3390/cryst13010093.

(13) Joannopoulos, J. D.; Johnson, S. G.; Winn, J. N.; Meade, R. D. *Photonic Crystals: Modelling the Flow of Light*, 2nd ed.; Princeton University of Press: Princeton, NJ, USA, 2008.

(14) Barkat, O. Theoretical Investigation of Transmission and Dispersion Properties of One-Dimensional Photonic Crystal. *J. Electr. Electron. Eng.* **2015**, 3 (2), 12−18, DOI: 10.11648/j.jeee.20150302.11.

(15) Shalaby, A. S.; Alamri, S.; Mohamed, D.; Aly, A. H.; Awasthi, S. K.; Matar, Z. S.; Tammam, M. T. for Theoretical study of one-dimensional defect photonic crystal as a high-performance sensor for water-borne bacteria. *Opt. Quantum Electron.* **2021**, *53*, No. 660, DOI: 10.1007/s11082-021-03291-2.

(16) Remler, R. F. The Solvent Properties of Acetone. *Ind. Eng. Chem.* **1923**, *15* (7), 717−720.

(17) Aljebory, A. Practical organic chemistry, 2013.

(18) Luttrell, W. E.; LaGrow, A. L. Acetone. *J. Chem. Health Saf.* **2014**, *21* (3), 29−31, DOI: 10.1016/j.jchas.2014.03.006.

(19) Hirschfelder, J. O.; Curtiss, C. F.; Bird, R. B. *Molecular Theory of Gases and Liquids*; Wiley: New York, 1954.

(20) Zaky, Z. A.; Ahmed, A. M.; Shalaby, A. S.; Aly, A. H. Refractive index gas sensor based on the Tamm state in a one-dimensional photonic crystal: Theoretical optimization. *Sci. Rep.* **2020**, No. 9736, DOI: 10.1038/s41598-020-66427-6.

(21) Upadhyay, M.; Lego, S. U. Refractive Index of Acetone-Water mixture at different concentrations. *Am. Int. J. Res. Sci., Technol., Eng. Math.* **2017**, *20* (1), 77−79.

(22) Singh, S. *Refractive Index Measurement, and its Applications*; IOP science, 2023.

(23) Gong, Y.; Kishi, R.; Kasai, S.; et al. Visual Dysfunction in Workers Exposed to a Mixture of Organic Solvents. *NeuroToxicology* **2003**, *24* (4−5), 703−710.

(24) Nowakowska, J. The Refractive Indices of Ethyl Alcohol and Water Mixtures. Mater Thesis; Loyola University Chicago, 1939.

(25) Chen, Y. H.; Shi, W. H.; Feng, L.; Xu, X. Y.; Shang-Guan, M. Y. Study on simultaneous sensing of gas concentration and temperature in one-dimensional photonic crystal. *Superlattices Microstruct.* **2019**, *131*, 53−58.

(26) Surdo, S.; Barillaro, G. On the performance of label-free biosensors based on vertical one-dimensional photonic crystal resonant cavities. *Opt. Express* **2015**, *23*, 9192−9201.

(27) Tassan, S.; Ferrari, G. M. A sensitivity analysis of the 'Transmittance−Reflectance' method for measuring light absorption by aquatic particles. *J. Plankton Res.* **2002**, *24* (8), 757−774.

(28) Kaňok, R.; Hlubina, P.; Gembalová, L.; Ciprian, D. Efficient optical sensing based on phase shift of waves supported by a one-dimensional photonic crystal. *Sensors* **2021**, *21*, No. 6535.

(29) Aly, A. H.; Awasthi, S. K.; Mohamed, D.; Matar, Z. S.; Al-Dossari, M.; Amin, A. F. Study on a one-dimensional defective photonic crystal suitable for organic compound sensing applications. *RSC Adv.* **2021**, *11* (52), 32973−32980.